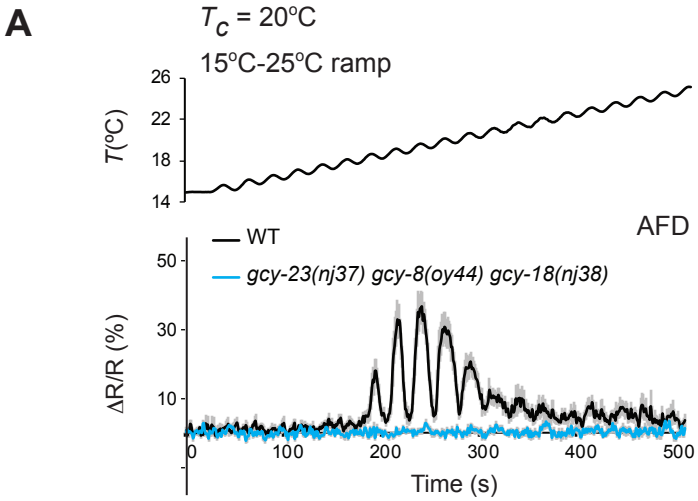

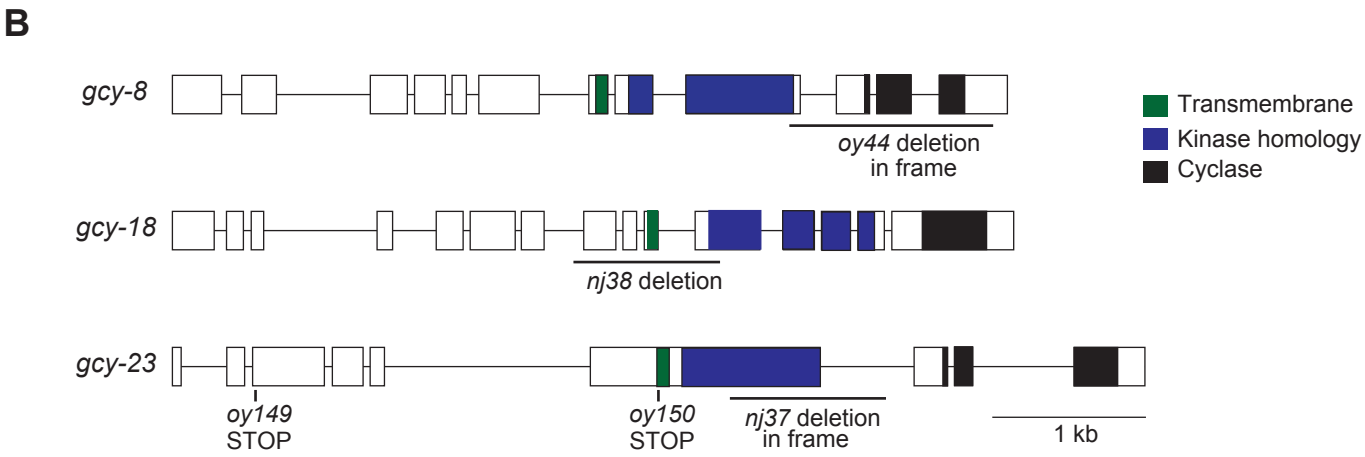

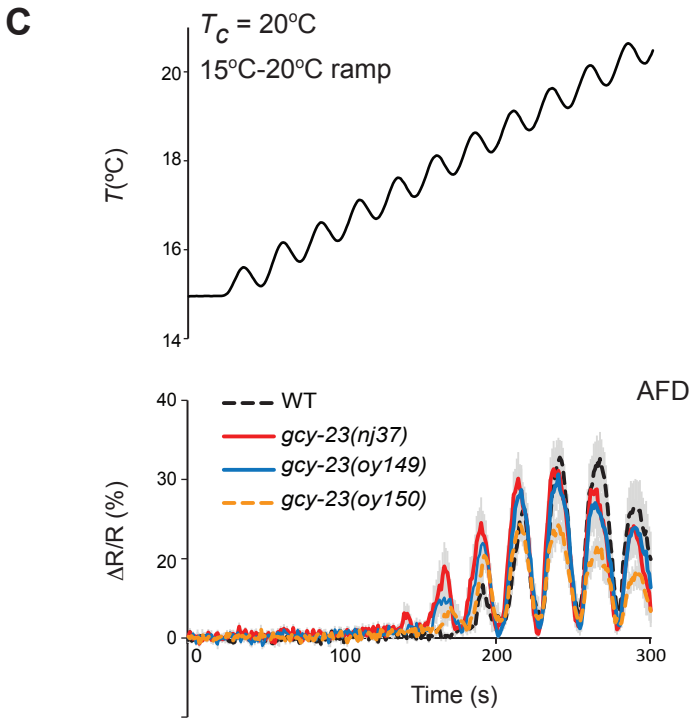

Takeishi, Yu et al, Figure S1 related to Figure 1

Figure S1 related to Figure 1. AFD-rGCs are necessary for thermotransduction in AFD.

A) Average ratiometric fluorescence changes in AFD neurons expressing YC3.6 in wild-type and *gcy-23(nj37) gcy-8(oy44) gcy-18(nj38)* mutants to the shown oscillating rising temperature ramp. The rate, frequency, and amplitude of temperature change was 0.02°C/sec, 0.04 Hz, and 0.5°C, respectively. Errors are SEM. n = 10 neurons each.

B) Predicted exon/intron structures of *gcy-8, gcy-18* and *gcy-23*. Filled boxes encode indicated domains. The locations and molecular nature of alleles used in this work are shown.

C) Average temperature-evoked ratiometric fluorescence changes in AFD neurons expressing cameleon YC3.6 in animals of the indicated genotypes. Errors are SEM. n=10 neurons each. T_c=20°C. The rate, frequency, and amplitude of temperature change was 0.02°C/sec, 0.04 Hz, and 0.5°C, respectively. Data for wild-type and *gcy-23(oy150)* animals are repeated from Figure 1 for comparison and are indicated by dashed lines.

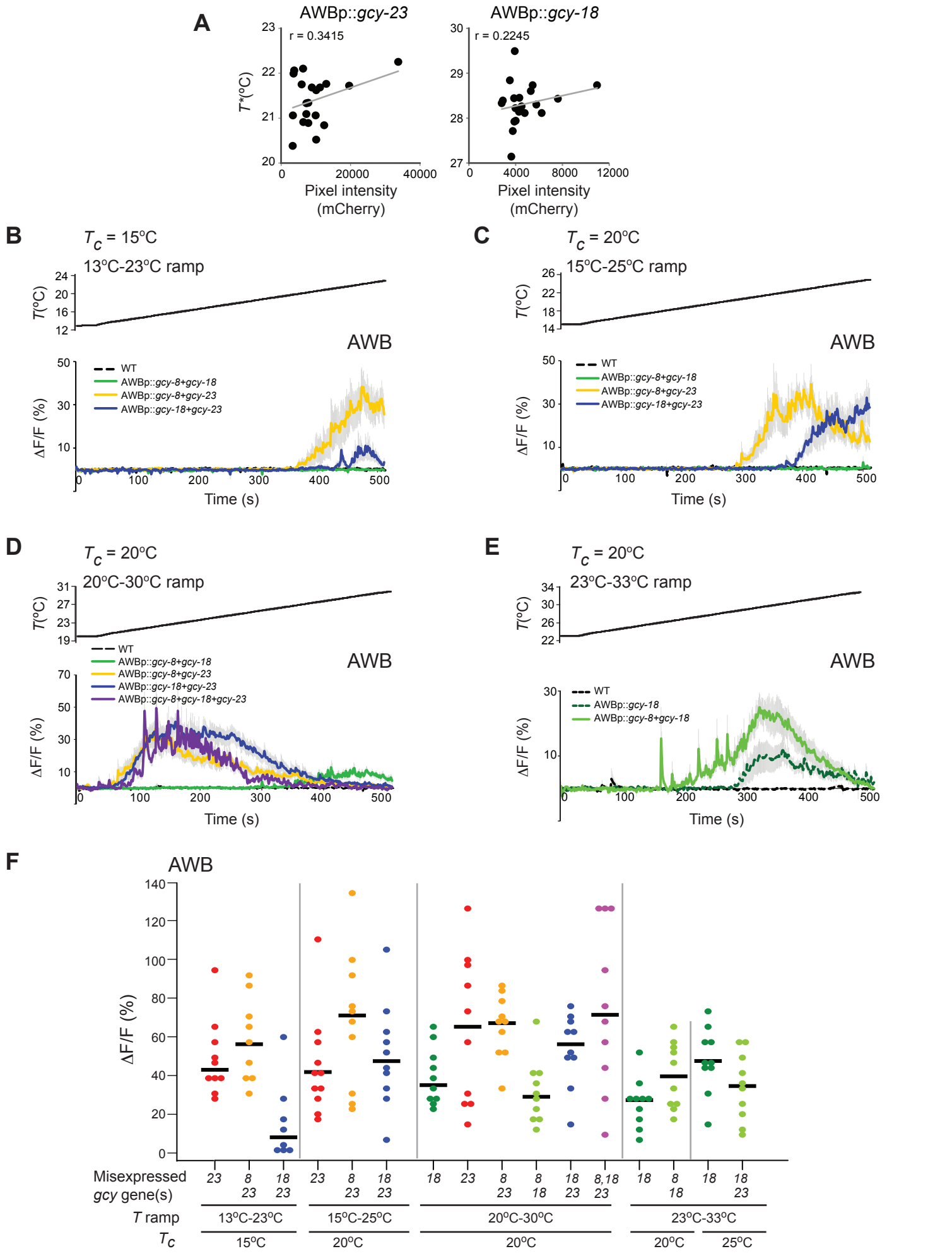

Takeishi, Yu et al Figure S2 related to Figures 3 and 4

Figure S2 related to Figures 3 and 4. Temperature responses conferred upon expression of AFD-rGCs in chemosensory neurons.

A) Correlation between mCherry fluorescence levels and T^* in individual AWB neurons (filled circles) expressing *rGC::SL2::mCherry*. *r* indicates the Pearson correlation coefficient. T_c=20°C; n=20 neurons each.

B-E) Average fluorescence changes in AWB neurons expressing GCaMP3 and/or the indicated genes to the shown rising temperature stimuli (black lines, 0.02°C/sec). *gcy* cDNAs were expressed under the *str-1* promoter in AWB, and coinjected at the same concentration each. Errors are SEM. n = 7-10 neurons each. All shown responses are averaged from two independent transgenic lines each. Peak response amplitudes of individual neurons are shown in **F**. Control data in **B-E** and *gcy-18* data in **E** are repeated from Figures 2 and 4 for comparison and are indicated by dashed lines.

F) Scatter plot of peak response amplitudes of individual neurons whose averaged responses are shown in Figures 3A-B, 4A-C and S2B-E. Horizontal black bars indicate medians. Response amplitudes are shown only for those strains in which responses above threshold (see Supplemental Experimental Procedures) were observed in one or more examined neurons.

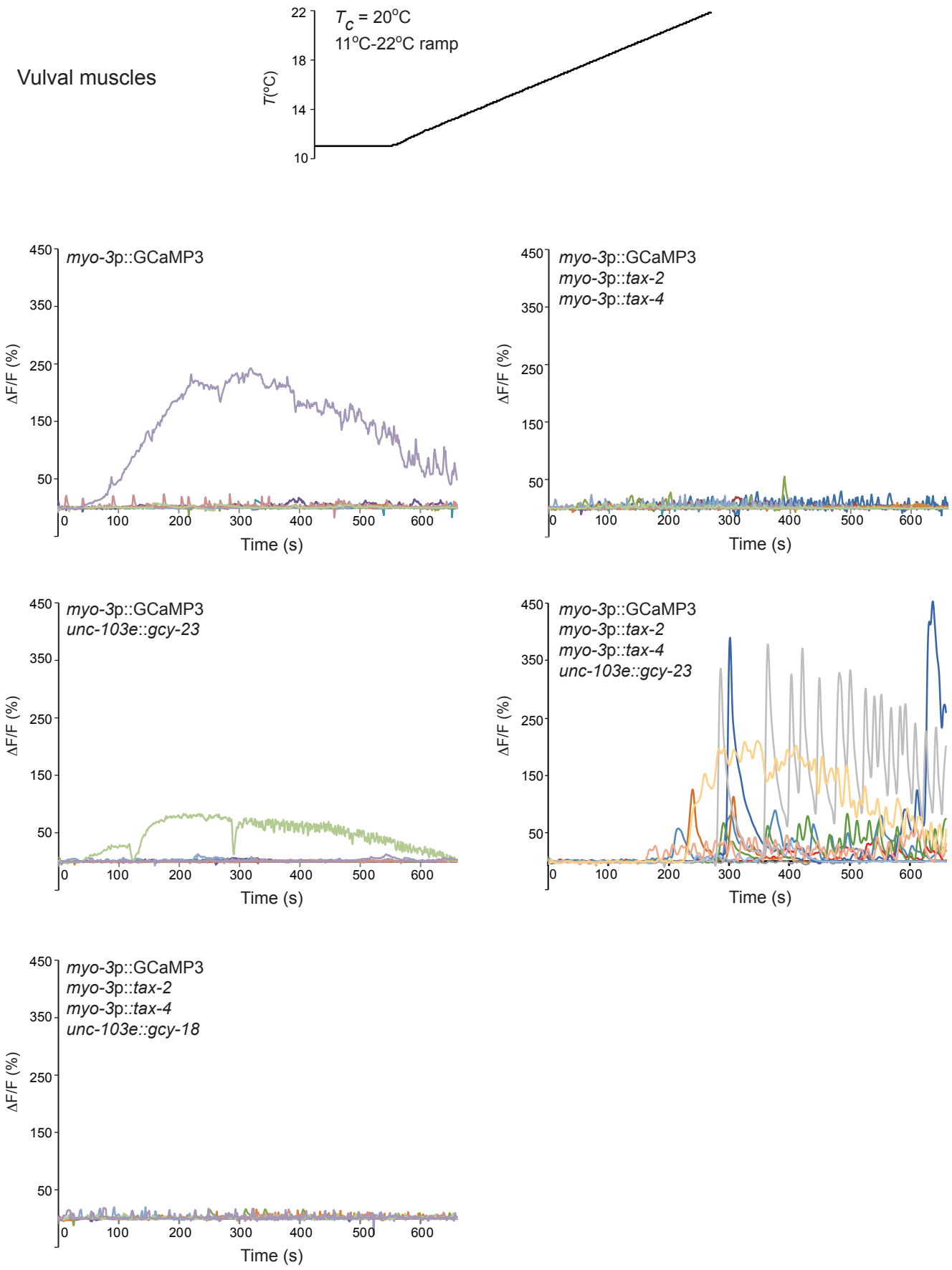

Takeishi, Yu et al, Figure S3 related to Figure 3

Figure S3 related to Figure 3. GCY-23 confers temperature responses upon ectopic expression in vulval muscles expressing TAX-2 and TAX-4.

Responses of individual animals expressing the indicated proteins in vulval muscles to the shown rising temperature stimulus (black line, 0.02°C/sec). Area under the curve during the first 60 seconds of the response are plotted in Figure 3D.

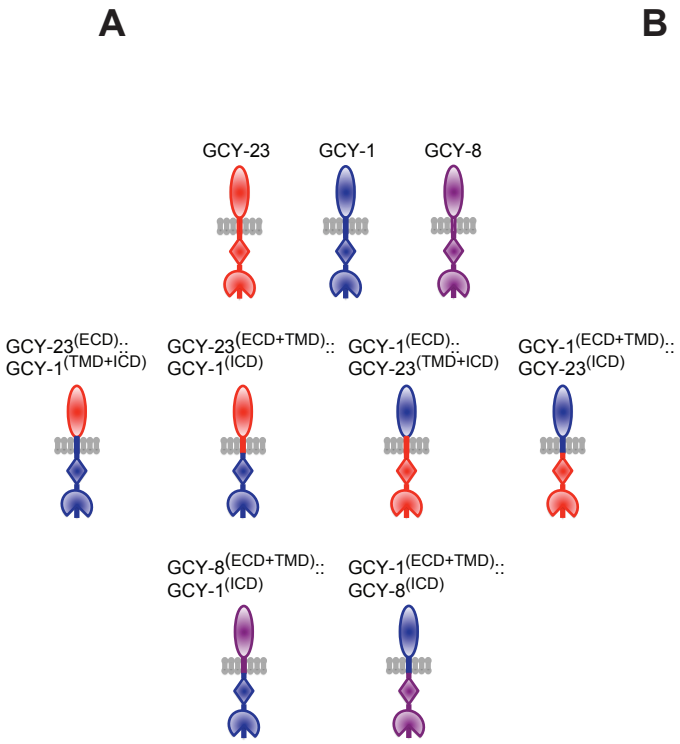

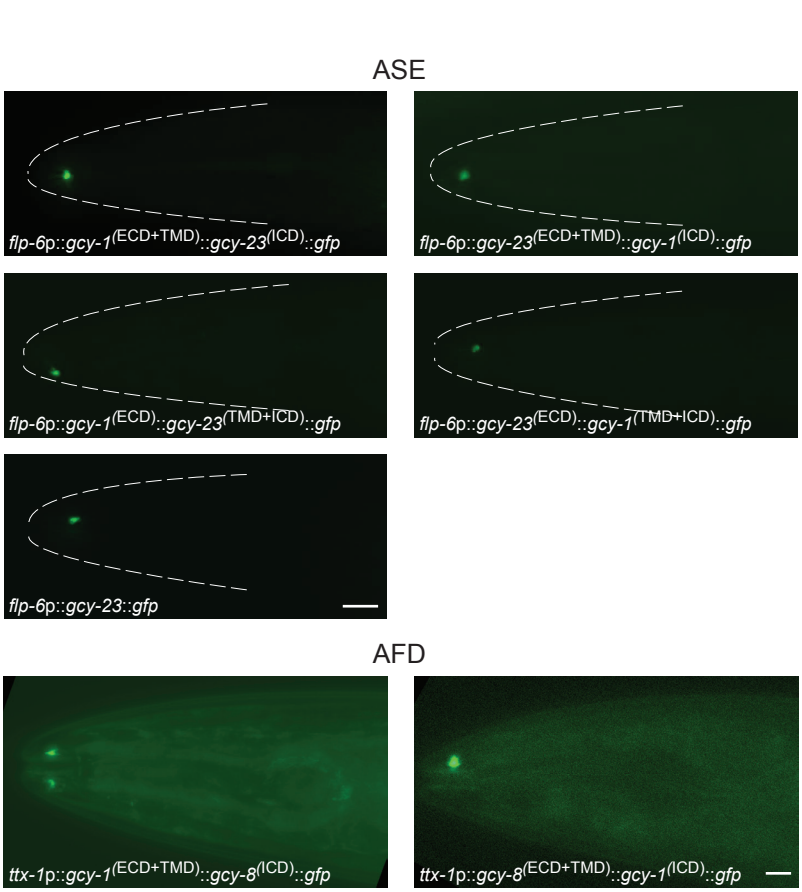

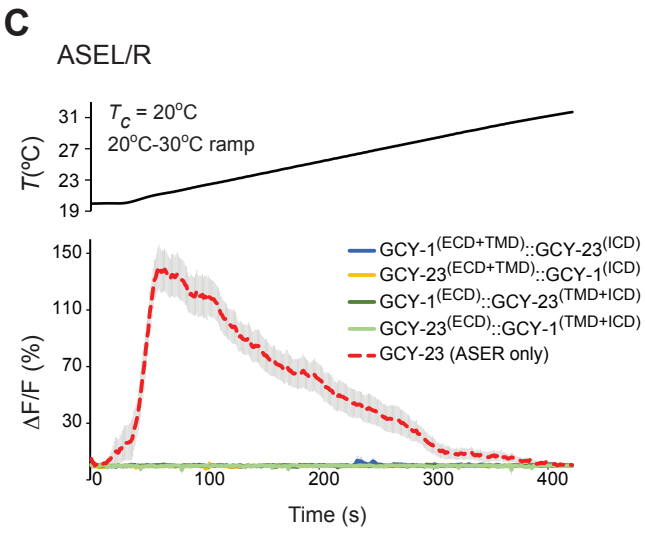

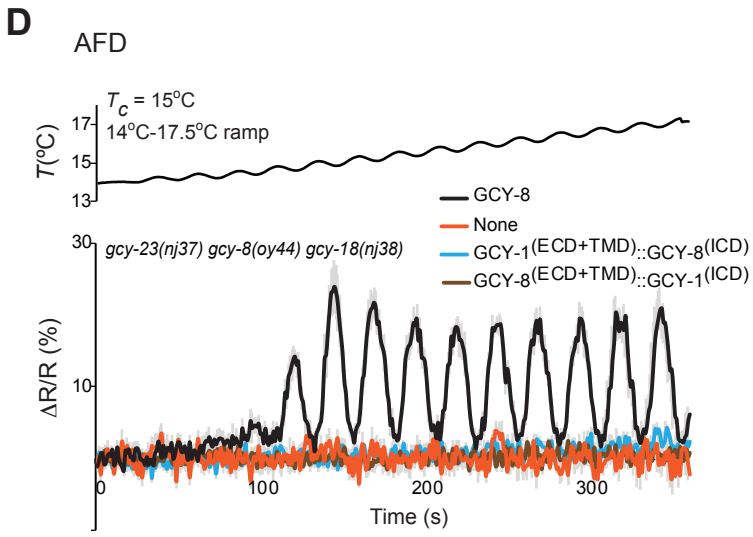

Takeishi, Yu et al Figure S4 related to Figure 4

Figure S4 related to Figure 4. Both the ICD and ECD domains may contribute to AFD-rGC thermosensory properties.

A) Cartoon representation of the domain organization of rGCs and rGC chimeric proteins as indicated in the legend to Figure 4D.

B) Localization of indicated chimeric proteins in ASE and AFD. Scale bars: 10 μm.

C) Average temperature-evoked fluorescence changes in ASEL/R neurons expressing GCaMP3 and the indicated rGC and rGC chimeric proteins. rGC and GCY-23::GCY-1 chimeric proteins were expressed under *flp-6* regulatory sequences. Errors are SEM. The rate of temperature change was 0.03°C/sec. All shown responses are averaged from at least two independent transgenic lines each. Responses of GCY-23 misexpressing neurons are repeated from Figure 4E for comparison purposes and are indicated by a dashed red line. n = 7-10 neurons each.

D) Average temperature-evoked ratiometric fluorescence changes in AFD neurons expressing cameleon YC3.6 in *gcy-23(nj37) gcy-8(oy44) gcy-18(nj38)* mutants expressing the indicated proteins under the *gcy-8* promoter. Errors are SEM. n=10 neurons each. T_c=15°C. The rate, frequency, and amplitude of temperature change was 0.01°C/sec, 0.04 Hz, and 0.2°C, respectively.

SUPPLEMENTAL MOVIE LEGENDS

Movie S1 related to Figure 2

Representative movie of temperature-evoked changes in GCaMP fluorescence in ASER neurons misexpressing *gcy-8*, *gcy-18* and *gcy-23*. T_c=20°C.

Movie S2 related to Figure 3

Representative movie of temperature-evoked changes in GCaMP fluorescence in AWB neurons misexpressing *gcy-23*. T_c=20°C.

Movie S3 related to Figure 3

Representative movie of temperature-evoked changes in GCaMP fluorescence in vulval muscles expressing *gcy-23*, *tax-2* and *tax-4*. T_c=20°C.

Table S1 related to Figures 1-4. The activation threshold (T^*) of AFD-rGCs is determined in a cell type-specific manner.

Misexpressed rGC[a] or *genotype*	Cell/Tissue	T_c (°C)	Temperature ramp (°C)	T^* (± SD)	*P*-value	T_{max} (± SD)[b]
WT	AFD	15	13-23	16.1 (0.5)		ND
WT	AFD	20	15-20	18.1 (0.3)	<0.001[c]	ND
GCY-8/18/23	ASEL	15	13-23	18.9 (0.8)		21.5 (0.4)
GCY-8/18/23	ASEL	20	15-25	20.5 (0.6)	<0.001[c]	22.1 (0.8)
GCY-8/18/23	ASER	15	13-23	19.1 (1.2)		21.5 (0.7)
GCY-8/18/23	ASER	20	15-25	20.4 (0.5)	0.007[c]	21.7 (0.5)
GCY-8/18/23	AWB	15	13-23	20.7 (0.6)		21.8 (0.6)
GCY-8/18/23	AWB	20	15-25	21.6 (0.5)	0.002[c]	22.7 (0.9)
GCY-8/18/23	AWB	20	20-30	21.4 (0.4)	0.006[c]	22.5 (1.0)
GCY-23	AWB	15	13-23	20.8 (0.8)		21.9 (0.7)
GCY-23	AWB	20	15-25	21.5 (0.4)	0.020[c]	22.4 (0.5)
GCY-23	ASER	15	13-23	18.5 (0.6)		20.8 (0.7)
GCY-23	ASER	20	15-25	20.0 (0.6)	<0.001[c]	21.5 (1.1)
GCY-23	AWB	20	20-30	21.0 (0.3)		22.4 (1.3)
GCY-18	AWB	20	20-30	28.6 (0.7)		29.5 (0.3)
GCY-18	ASER	20	20-30	28.2 (0.5)		29.8 (0.2)
GCY-18	AWB	15	23-33	28.8 (0.6)		29.7 (0.9)
GCY-18	AWB	20	23-33	29.6 (1.2)	0.077[c]	30.4 (1.1)
GCY-8/23	AWB	15	13-23	21.1 (0.8)	0.458[d]	22.0 (0.7)
GCY-8/23	AWB	20	15-25	21.4 (0.7)	0.769[d]	22.5 (0.7)
GCY-8/23	AWB	20	20-30	21.1 (0.4)	0.664[d]	21.9 (0.6)
GCY-8/18	AWB	20	20-30	27.1 (0.8)	<0.001[e]	28.2 (0.6)
GCY-8/18	AWB	20	23-33	27.0 (0.8)	<0.001[e]	28.2 (1.5)
GCY-18/23	AWB	15	13-23	20.9 (0.8)	0.875[d,f]	22.1 (0.4)[f]
GCY-18/23	AWB	20	15-25	22.9 (0.8)	<0.001[d]	24.1 (0.8)
GCY-18/23	AWB	20	20-30	21.2 (0.4)	0.326[d], <0.001[e]	22.7 (0.7)
GCY-18	AWB	25	23-33	28.8 (0.6)		29.5 (0.5)
GCY-18/23	AWB	25	23-33	26.3 (1.7)	<0.001[e]	28.8 (1.6)
GCY-23	VM	20	11-22	14.1 (1.0)		ND
gcy-8(oy44)	AFD	20	15-20	17.5 (0.2)	<0.001[g]	ND
gcy-18(nj38)	AFD	20	15-20	18.0 (0.4)	0.377[g]	ND
gcy-23(nj37)	AFD	20	15-20	17.9 (0.4)	0.377[g]	ND
gcy-23(oy149)	AFD	20	15-20	18.0 (0.4)	0.433[g]	ND
gcy-23(oy150)	AFD	20	15-20	18.1 (0.4)	0.991[g]	ND
gcy-23(oy150) gcy-8(oy44)	AFD	20	15-20	17.5 (0.6)	0.005[g]	ND
gcy-23(oy150) gcy-18(nj38)	AFD	20	15-20	16.9 (0.2)	<0.001[g]	ND
gcy-8(oy44) gcy-18(nj38)	AFD	20	15-20	17.0 (0.3)	<0.001[g]	ND
GCY-23	ASER	20	20-32	20.1 (0.0)		21.2 (0.2)
GCY-18	ASER	20	20-32	28.5 (0.3)		30.6 (0.8)
GCY-$23^{(ECD)}$::GCY-	ASER	20	20-32	31.0 (0.2)		32.6 (0.3)

$18^{(TMD+ICD)}$					
GCY-$23^{(ECD+TMD)}$::GCY-$18^{(ICD)}$	ASER	20	20-32	27.6 (0.3)	29.9 (1.0)
GCY-$18^{(ECD)}$::GCY-$23^{(TMD+ICD)}$	ASER	20	20-32	25.5 (0.3)	27.7 (1.4)
GCY-$18^{(ECD+TMD)}$::GCY-$23^{(ICD)}$	ASER	20	20-32	27.5 (0.4)	28.5 (0.8)

[a]rGCs were ectopically expressed under the following promoters: ASEL/R – *flp-6*; ASER- *gcy-5*; AWB – *str-1*; vulval muscles (VM) – *unc-103e*.
[b]T_{max} indicates the average temperature of peak response amplitude.
[c]As compared to values at 15°C in the same genetic background.
[d]As compared to values under the same conditions in neurons expressing GCY-23 alone.
[e]As compared to values under the same conditions in neurons expressing GCY-18 alone.
[f]Calculated from the subset of responding neurons (Figure S2F).
[g]As compared to values in wild-type animals under the same conditions.
n=7-10 neurons from at least two transgenic lines for each. ND – not done.

Table S2 related to all Figures. List of strains used in this work.

See Excel File.

SUPPLEMENTAL EXPERIMENTAL PROCEDURES

C. elegans strains

The wild-type strain was *C. elegans* variety Bristol, strain N2. Strains were maintained with *E. coli* OP50 as the food source. Transgenic animals were generated using test plasmids at 1-60 ng/µl and the *unc-122*p*::gfp, unc-122*p*::rfp* or *ttx-3*p*::gfp* coinjection markers at 30 or 50 ng/µl. Strains expressing genetically encoded calcium indicators were the following: PY9735 (*str-1*p::*GCaMP3*); ZC1600 (*flp-6*p::*GCaMP3*) (Luo et al., 2014)); PY8971 (*srtx-1*p::*YC3.6*) (Yu et al., 2014)); PY8339 (*gcy-8*p::*GCaMP3)*; AQ2364 (*myo-3*p::*GCaMP3*) (gift from W. Schafer) (Butler et al., 2015). The presence of specific mutations in a strain was confirmed by sequencing. A complete list of all strains used in this work is provided in Table S2.

Molecular biology

gcy cDNAs were amplified from a *C. elegans* cDNA library generated from a population of mixed stage animals, and verified via sequencing. To facilitate identification of transgenic animals misexpressing the rGCs in the appropriate cell type, rGC cDNAs were fused via a SL2 trans-splicing leader sequence to a *mCherry* reporter. *gcy* cDNAs were misexpressed under the following gene regulatory sequences: AWB – *str-1* (2.4 or 3.0 kb); ASEL/R – *flp-6* (2.7 kb), ASER - *gcy-5* (3.2 kb). The *gcy-23* and *gcy-18* cDNAs were expressed in vulval muscles under the *unc-103e* regulatory sequences (Reiner et al., 2006) (gift of K. Shen); *tax-2* and *tax-4* cDNAs were expressed under the *myo-3* promoter (2.5 kb). The sequence change encoding the D927A mutation in the *gcy-23* cDNA was introduced via PCR-based mutagenesis and confirmed by sequencing.

To generate GFP-tagged GCY proteins, sequences encoding GFP were introduced just prior to the STOP codon in the *gcy* cDNAs and the fusion genes were expressed under *srd-23, flp-6*, or *ttx-1* upstream regulatory sequences for expression in AWB, ASE, and AFD, respectively. Chimeric constructs between different *gcy* genes were generated using the Gibson assembly method (Gibson et al., 2009). Overlapping amplicons from different *gcy* genes were assembled with a linearized expression vector using the NEBuilder HiFi DNA assembly master mix. Constructs were verified via sequencing. Transmembrane domains of each GCY protein were predicted by the Simple Modular Architecture Tool (http://smart.embl-heidelberg.de/). The junction sites in each rGC are as follows (amino acid residues included in each domain are indicated in parentheses):

GCY-1: ECD(1-496), TMD(497-519), ICD(520-1137)

GCY-8: ECD(1-504), TMD(505-527), ICD(528-1152)

GCY-18: ECD(1-497), TMD(498-520), ICD(521-1113)

GCY-23: ECD(1-457), TMD(458-480), ICD(481-1073)

Chimeric constructs were expressed in ASE and AFD under *flp-6* or *gcy-5,* and *gcy-8,* regulatory sequences, respectively.

Generation of a *gcy-23* null allele via CRISPR/Cas9-mediated gene editing

The *gcy-23(oy149)* and *gcy-23(oy150)* alleles were generated via CRISPR/Cas9-mediated gene editing as described (Arribere et al., 2014; Paix et al., 2014; Zhao et al., 2014). In brief, *gcy-23* sgRNA sequences and *rol-6(su1006)* sgRNA sequences (Arribere et al., 2014; Friedland et al., 2013) were injected (at 25 ng/μl each) together with *gcy-23* and *rol-6(su1006)* oligonucleotides (at 500 nM each), and the Cas9-encoding plasmid

pDD162 (at 50 ng/µl) (Dickinson et al., 2013) into *gcy-8(oy44) gcy-18(nj38)* animals (Inada et al., 2006). F1 roller animals were isolated, and the presence of mutations in the *gcy-23* sequence was confirmed by amplification and sequencing. F2 non-roller progeny were further screened for the presence of the homozygous *gcy-23* mutation. Sequences of the *gcy-23* sgRNA and *gcy-23* donor oligonucleotides are provided below. Sequences of the *rol-6* sgRNA and *rol-6* oligonucleotides have been previously described (Arribere et al., 2014).

gcy-23(oy149) sgRNA: 5'- ATCCTGAACCAAATGGGATG – 3'

gcy-23(oy150) sgRNA: 5'- GCATCCTCCGATAATCAATG – 3'

gcy-23(oy149) oligonucleotide: 5' –
CTAGAACCTGTAATGTTTTCAGAATCCTGAACCAAATGGGTAAATAAATAAG
CAAAGAATCGTATGAAGGTGTTGCGGTAAGTGCAGACATGTACCATGTTCAA
GGAGTTCGTGCATTT -3'

gcy-23(oy150) oligonucleotide: 5' –
CAGAAGTACAATGCATCCTCCGATAATCATTATTTATTTATGTAATGTAGTCG
CATTTTTCATTTCGGAA -3''

***in vivo* calcium imaging**

Ca^{2+} imaging experiments were performed essentially as described previously (Yu et al., 2014). Imaging was performed in animals expressing the genetically encoded calcium indicators GCaMP3 in AWB, ASE, AFD, and muscle, or yellow cameleon YC3.6 in AFD (Clark et al., 2007; Wasserman et al., 2011; Yu et al., 2014). Misexpressing cells were identified via the expression of SL2::mCherry; animals

expressing similar levels of mCherry were selected for imaging to control for gene expression. To control for variability in expression of the calcium indicator (Hires et al., 2008), we only imaged animals expressing the indicator within an expression range defined experimentally for each cell type. Fluorescence intensities in the soma were quantified using ImageJ (NIH) software. Growth-synchronized L4 larval stage animals were cultivated overnight at specific temperatures, and young adults were imaged the next day for somal or vulval muscle calcium responses to temperature stimuli.

Individual animals were placed on a 10% agarose pad on a coverslip and immobilized with 1.5 μl of 2.5% (w/v) solution of 0.1 μm polystyrene beads (Polysciences), or freshly prepared 10 mM levamisole (Sigma Aldrich), and covered with a second glass coverslip. Sandwiched coverslips and animals were transferred and mounted with 5 μl of glycerol on a glass slide secured onto a Peltier on the microscope stage prewarmed to the desired starting temperature. Current delivery was controlled by temperature-regulated feedback using LabView (National Instruments) to achieve the desired target temperature; the temperature was measured using a 15K thermistor (McShane Inc). Animals were subjected to temperature ramps with 0.01°C/sec - 0.03°C/sec rates of temperature change as indicated in the figure legends. For imaging in AFD, a sinusoidal oscillation of 0.04 Hz and and 0.2°C-0.5°C amplitude was superimposed upon the linear temperature ramp to facilitate detection of T^*_{AFD} using the YC3.6 calcium indicator (Clark et al., 2006). Calcium dynamics in vulval muscles were initially assessed in response to different temperature stimuli in order to identify the responding range; all subsequent experiments were performed using the responding

temperature range. Baseline fluorescence was set to zero to offset fluorescence decreases caused by photobleaching or movement artifacts.

Images were captured using a Zeiss 40X air objective (NA 0.9) using MetaMorph software (Molecular Devices), and a digital camera (Orca, Hamamatsu) at a rate of 1 Hz. Data were analyzed using custom written scripts in MATLAB. T^* was defined as the temperature at which ΔF/F increased by a minimum of 2% over at least 8 consecutive seconds with an average slope of >0.3% per sec. In vulval muscles, T^* was defined as the temperature at which ΔF/F increased by >30%. For cells expressing YC3.6, T^* was defined as the temperature at which the YFP/CFP ratio first phase-locked to the sinusoidal variation in the stimulus. All shown responses are pooled and averaged from at least two independent transgenic lines each.

Q_{10} measurements

Since temperature-evoked calcium responses as detected by changes in GCaMP fluorescence saturate (Hires et al., 2008), we performed all measurements in a narrow temperature range around the corresponding T^* for each neuron. Q_{10} values were calculated from peak normalized fluorescence values ($\Delta F_{peak}/F$) obtained in response to five successive temperature transients (ΔT = 0.4°C, 0.8°C, 1.2°C, 0.8°C, 0.4°C) from a constant holding temperature (T_{hold}). Repeat measures at the lower and middle nominal temperature transients (ΔT = 0.4°C, 0.8°C) were averaged. The T_{hold} was selected as a temperature that was ~0.5°C higher than T^* for each neuron type under the examined conditions (T_c=20°C; AFD T_{hold} = 19.0°C; AWB T_{hold} = 22.1°C). We estimated Q_{10} using

the slope parameters of a mixed-effects linear model fitted to $\log(\Delta F_{peak}/F)$ with the unit of replication (animal, n=10 in all cases) as a random effect and ΔT as a fixed effect.

Behavior

Animals were cultivated overnight at 15ºC with food. Prior to the start of the assay, 15 young adult animals were transferred to a 10 cm unseeded NGM plate pre-chilled at 15ºC, which was in turn placed on an aluminum plate with the temperature set at 15ºC. The temperature on the aluminum plate was established and maintained by Peltier thermoelectric temperature controllers (Oven Industries). The temperature of the NGM plate was measured with a two probe digital thermometer (Fluke Electronics). Animals were assayed for locomotion on plates held at 15ºC for 15 min following which the temperature of the aluminum plate was raised to 28ºC or maintained at 15ºC for the remainder of the experiment. Animal movement was recorded at a rate of 1 Hz using a PixeLink CCD camera. Videos were analyzed using custom written scripts in MATLAB. A turn was defined as an instantaneous change in direction greater than 27.7ºC from the average run direction.

REFERENCES

Arribere, J.A., Bell, R.T., Fu, B.X., Artiles, K.L., Hartman, P.S., and Fire, A.Z. (2014). Efficient marker-free recovery of custom genetic modifications with CRISPR/Cas9 in *Caenorhabditis elegans*. Genetics *198*, 837-846.

Butler, V.J., Branicky, R., Yemini, E., Liewald, J.F., Gottschalk, A., Kerr, R.A., Chklovskii, D.B., and Schafer, W.R. (2015). A consistent muscle activation strategy underlies crawling and swimming in *Caenorhabditis elegans*. J. R. Soc. Interface *12*, 20140963.

Dickinson, D.J., Ward, J.D., Reiner, D.J., and Goldstein, B. (2013). Engineering the *Caenorhabditis elegans* genome using Cas9-triggered homologous recombination. Nat. Methods *10*, 1028-1034.

Friedland, A.E., Tzur, Y.B., Esvelt, K.M., Colaiacovo, M.P., Church, G.M., and Calarco, J.A. (2013). Heritable genome editing in *C. elegans* via a CRISPR-Cas9 system. Nat. Methods *10*, 741-743.

Gibson, D.G., Young, L., Chuang, R.Y., Venter, J.C., Hutchison, C.A., 3rd, and Smith, H.O. (2009). Enzymatic assembly of DNA molecules up to several hundred kilobases. Nat. Methods *6*, 343-345.

Hires, S.A., Tian, L., and Looger, L.L. (2008). Reporting neural activity with genetically encoded calcium indicators. Brain Cell Biol. *36*, 69-86.

Inada, H., Ito, H., Satterlee, J., Sengupta, P., Matsumoto, K., and Mori, I. (2006). Identification of guanylyl cyclases that function in thermosensory neurons of *Caenorhabditis elegans*. Genetics *172*, 2239-2252.

Luo, L., Wen, Q., Ren, J., Hendricks, M., Gershow, M., Qin, Y., Greenwood, J., Soucy, E.R., Klein, M., Smith-Parker, H.K.*, et al.* (2014). Dynamic encoding of perception, memory, and movement in a *C. elegans* chemotaxis circuit. Neuron *82*, 1115-1128.

Paix, A., Wang, Y., Smith, H.E., Lee, C.Y., Calidas, D., Lu, T., Smith, J., Schmidt, H., Krause, M.W., and Seydoux, G. (2014). Scalable and versatile genome editing using linear DNAs with microhomology to Cas9 Sites in *Caenorhabditis elegans*. Genetics *198*, 1347-1356.

Reiner, D.J., Weinshenker, D., Tian, H., Thomas, J.H., Nishiwaki, K., Miwa, J., Gruninger, T., Leboeuf, B., and Garcia, L.R. (2006). Behavioral genetics of *Caenorhabditis elegans unc-103*-encoded erg-like K(+) channel. J. Neurogenet. *20*, 41-66.

Yu, Y.V., Bell, H.W., Glauser, D.A., Goodman, M.B., Van Hooser, S.D., and Sengupta, P. (2014). CaMKI-dependent regulation of sensory gene expression mediates experience-dependent plasticity in the operating range of a thermosensory neuron. Neuron *84*, 919-926.

Zhao, P., Zhang, Z., Ke, H., Yue, Y., and Xue, D. (2014). Oligonucleotide-based targeted gene editing in *C. elegans* via the CRISPR/Cas9 system. Cell Res. *24*, 247-250.